Kinetics and Energetics of Subunit Dissociation/Unfolding of TIM: The Importance of Oligomerization for Conformational Persistence and Chemical Stability of Proteins†

Alex W. M. Rietveld* and Sérgio T. Ferreira

Departamento de Bioquímica Médica, Instituto de Ciências Biomédicas, Universidade Federal do Rio de Janeiro, Rio de Janeiro, RJ 21941-590, Brazil

Received August 29, 1997; Revised Manuscript Received October 29, 1997⊗

ABSTRACT: Kinetics of unfolding and refolding of rabbit muscle triosephosphate isomerase (TIM) were measured as a function of guanidine hydrochloride (GdnHCl) concentration. From the rate constants of these processes, the activation free-energy barriers ($\Delta G^{\ddagger}$) were calculated using the Arrhenius equation. Assuming a linear dependence of $\Delta G^{\ddagger}$ on the concentration of GdnHCl, activation energies in the absence of GdnHCl were estimated. The Gibbs free-energy change of dissociation/unfolding (ΔG) was determined from GdnHCl unfolding curves in equilibrium. Using these data and the literature value for the bimolecular association rate constant of folded TIM monomers [Zabori, S., Rudolph, R., and Jaenicke, R. (1980) *Z. Naturforsch. 35C,* 999−1004], a model was developed that fully describes both kinetics and energetics of subunit dissociation/unfolding of TIM. Unfolded TIM monomers are susceptible to proteolytic digestion and thiol oxidation, while native TIM is resistant to both. The present model explains how the dimeric nature of TIM decreases the frequency of subunit unfolding by several orders of magnitude, thus increasing the chemical stability of the protein. Furthermore, the model also explains the recently demonstrated persistence (on a time scale of hours to days) of conformational heterogeneity of native TIM dimers [Rietveld, A. W. M., and Ferreira, S. T. (1996) *Biochemistry 35,* 7743−7751]. Again, it appears that the dimeric nature of TIM is essential for this behavior.

TIM[1] is a glycolytic enzyme that interconverts D-glyceraldehyde 3-phosphate and dihydroxyacetone phosphate. Crystal structures for TIM from various organisms have been determined (chicken, yeast, *Trypanosoma brucei*, *Escherichia coli*, human, *Bacillus stearothermophilus*; refs *1*−*6*). Both primary (*6*) and three-dimensional (*7*) structures of TIM show a high degree of conservation. TIM is a homodimer of approximately 26 kDa subunits, and each subunit consists of a single eight-stranded $\alpha\beta$-barrel domain.

The kinetics of refolding of TIM after unfolding induced by guanidine hydrochloride (GdnHCl) have been investigated (*8*, *9*). Refolding appears to proceed from unfolded monomers to folded, inactive monomers, and then to native, active dimers. TIM mutants that form folded, inactive monomers have been produced (*10*, *11*).

Native TIM is resistant to digestion by various proteases, while unfolded TIM loses this stability (*8*, *12*). In addition, native TIM contains several reduced cysteine residues and no disulfide bridges. Analysis of TIM crystal structures shows that the cysteine residues are quite far apart in the structure, effectively preventing disulfide formation. On the other hand, unfolded TIM is susceptible to sulfhydryl oxidation (*13*). These observations indicate that the chemical stability of TIM is closely related to its conformational stability.

Using hydrostatic pressure as a tool to perturb the equilibrium of subunit association of TIM, we have shown a lack of dependence of dissociation/unfolding on protein concentration (*13*). This is an apparent violation of the law of mass action, according to which dissociation of an oligomer into its constituent subunits should depend in a predictable manner on protein concentration. Similar observations have been made for subunit dissociation of large protein aggregates such as viral particles (ref *14*, and references therein) and have been explained as deterministic behavior arising from persistent conformational heterogeneity in the ensemble of native oligomers (*15*). For TIM, persistent heterogeneity in pressure-sensitivity has been demonstrated, and it was proposed to originate from conformational heterogeneity of the dimers (*13*). A prerequisite for such heterogeneity is that the dynamics of subunit exchange/unfolding should be slow relative to the experimental time scale (*i.e.*, hours or longer). Conceivably, the conformational persistence of TIM allows subtle conformational differences between TIM dimers to last during this time scale, giving them individual, pre-determined character, comparable to the behavior of macromolecular bodies (*13*, *15*).

† This paper is dedicated to the memory of Prof. Gregorio Weber, whose work and support have inspired much of this research. Supported by grants from Financiadora de Estudos e Projetos, Conselho Nacional de Desenvolvimento Científico e Tecnológico, Fundação de Amparo à Pesquisa do Estado do Rio de Janeiro, and Howard Hughes Medical Institute. S.T.F. is a Howard Hughes Medical Institute International Research Scholar. A.W.M.R. is recipient of a fellowship from Coordenação de Aperfeiçoamento de Pessoal Docente de Ensino Superior.

* Author to whom correspondence should be addressed. Telephone: (+5521)270-5988. Fax: (+5521)270-8647. E-mail: rietveld@bioqmed.ufrj.br.

⊗ Abstract published in *Advance ACS Abstracts,* December 15, 1997.

[1] Abbreviations: GdnHCl, guanidine hydrochloride; TIM, triosephosphate isomerase.

S0006-2960(97)02159-4 CCC: $15.00
Published on Web 01/20/1998

In the present study, kinetics and energetics of both association/dissociation and (un)folding of rabbit TIM were examined. Unfolding and refolding were measured as a function of GdnHCl concentration. By extrapolation to absence of GdnHCl and the use of literature values for the bimolecular association rate constant of TIM monomers (*9*), a model is presented that gives a comprehensive description of both kinetics and energetics of subunit dissociation and unfolding of TIM.

MATERIALS AND METHODS

Materials. Rabbit muscle triosephosphate isomerase (TIM, type X), guanidine hydrochloride, dithiothreitol, and phosphate buffer were from Sigma.

Fluorescence Measurements. All experiments were carried out in 50 mM phosphate buffer, pH 7.4, containing 1 mM dithiothreitol, with protein concentrations as indicated in the legends to the figures. Fluorescence data were acquired on an automated ISS PC1 spectrofluorometer (ISS Inc., Champaign, IL). Temperature was kept constant at 25 ± 0.3 °C by means of a circulating bath.

For equilibrium unfolding experiments, samples were equilibrated for 3 days at 25 °C in the presence of the indicated concentrations of GdnHCl. Spectra were measured from 300 to 400 nm ($\lambda_{exc} = 280$ nm) with 8 nm bandpasses for both excitation and emission. Fluorescence spectral centers of mass at each concentration of GdnHCl ($\lambda_{[GdnHCl]}$) were calculated with software provided by ISS Inc. as

$$\lambda_{[GdnHCl]} = \frac{\sum \lambda I(\lambda)}{\sum I(\lambda)} \quad (1)$$

where λ is the emission wavelength and $I(\lambda)$ is the fluorescence intensity at wavelength λ.

In unfolding/refolding kinetics experiments, samples were excited at 280 nm (16 nm bandpass) through a Corning 7-54 filter and fluorescence emission was collected through a Schott WG 335 filter. Unfolding was initiated by adding native TIM to a solution containing the desired concentration of GdnHCl. For refolding experiments, TIM was first unfolded for at least 20 min (which was determined to be sufficient for equilibration; see Results) in 3 M GdnHCl, and aliquots were diluted in buffer containing the appropriate concentration of GdnHCl. All samples were bubbled with a stream of nitrogen and placed in sealed cuvettes prior to measurements.

Data Fitting. Equilibrium unfolding experiments were analyzed by assuming that the free-energy change (ΔG) for the equilibrium between native dimers and unfolded monomers is linearly affected by GdnHCl (*16*). The dissociation/unfolding equilibrium constant K_0 and the *m* value (the slope of the free-energy change as a function of GdnHCl concentration) were obtained by fitting eqs 2 and 3 to the experimental data:

$$\lambda_{[GdnHCl]} = \lambda_0 + \Delta\lambda\left(\frac{K_{[GdnHCl]}}{4[TIM] + K_{[GdnHCl]}}\right) \quad (2)$$

where λ_0 is the spectral center of mass of native TIM, $\Delta\lambda$ is the total change in spectral center of mass upon complete dissociation/unfolding, [TIM] is the concentration of TIM (in monomers), and $K_{[GdnHCl]}$ is the dissociation/unfolding constant at a given concentration of GdnHCl, given by

$$K_{[GdnHCl]} = K_0 \exp\left(\frac{m[GdnHCl]}{RT}\right) \quad (3)$$

Fitting parameters in this model are λ_0, $\Delta\lambda$, K_0, and *m*. In initial fits, *m* was used as a free fitting parameter, and similar *m* values were obtained for data obtained at two different protein concentrations. In order to allow direct comparison of the fitted values for K_0 at different protein concentrations, in final fits *m* was fixed at the average value obtained from the initial fits. The fluorescence quantum yields of native and fully unfolded TIM were approximately the same; therefore, no correction due to this factor was required in the fits. Furthermore, independent experiments showed that the spectra of both folded dimeric and unfolded monomeric TIM (*i.e.*, below and above the transition regions, respectively) were negligibly dependent on GdnHCl concentration (data not shown). Therefore, we did not correct for direct effects of GdnHCl on the fluorescence spectral shift (a correction that was included in the original fitting procedure of Pace, ref *16*). The extent of dissociation/unfolding (α) at each concentration of GdnHCl was calculated using the values for λ_0 and $\Delta\lambda$ recovered from the fits:

$$\alpha = \frac{\lambda_{[GdnHCl]} - \lambda_0}{\Delta\lambda} \quad (4)$$

For kinetic experiments, rate constants of unfolding/refolding were obtained by fitting a mono-exponential equation to the data:

$$I_t = I_0 + \Delta I \exp(-kt) \quad (5)$$

where I_t is the fluorescence intensity at time *t*, I_0 is the fluorescence intensity of the initial state (either folded or unfolded), ΔI is the total intensity change in unfolding or refolding, and *k* is the rate constant of the reaction. Degrees of dissociation/unfolding (α) were calculated as

$$\alpha = \frac{I_t - I_0}{\Delta I} \quad (6)$$

Activation free-energies ($\Delta G^{\ddagger}$) were calculated using the Arrhenius equation

$$k = (k_b T/h) \exp(-\Delta G^{\ddagger}/RT) \quad (7)$$

where k_b is Boltzman's constant and *h* is Planck's constant. Extrapolation to absence of GdnHCl was obtained by assuming a linear dependence of $\Delta G^{\ddagger}$ on the concentration of GdnHCl (*17*−*19*):

$$\Delta G^{\ddagger}_{[GdnHCl]} = \Delta G^{\ddagger}_0 + m^{\ddagger}[GdnHCl] \quad (8)$$

RESULTS

Figure 1 shows equilibrium dissociation/unfolding of TIM as a function of GdnHCl concentration at two different protein concentrations. The unfolding curves featured the following characteristics.

(1) Dependence of unfolding on protein concentration was observed, as expected from the law of mass action for a

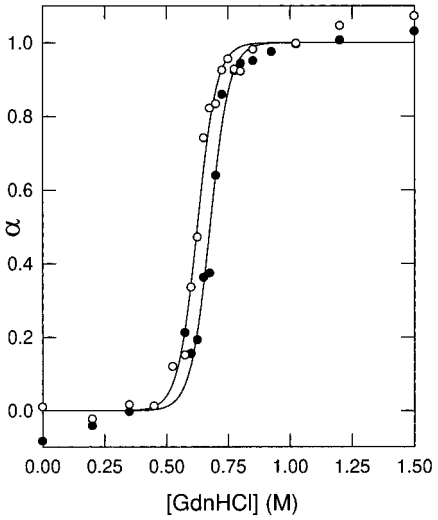

FIGURE 1: Equilibrium subunit dissociation/unfolding of TIM by GdnHCl at two different protein concentrations. Protein concentrations were 6 μM (closed circles) and 0.6 μM (open circles). Lines represent fits according to eqs 2 and 3.

Table 1: Equilibrium Subunit Dissociation/Unfolding of TIM by GdnHCl[a]

[TIM] (μM)	λ_0 (nm)	$\Delta\lambda$ (nm)	K_0 (10^{-13} M)	m (kJ mol^{-1} M^{-1})	ΔG (kJ/mol)
0.6	334.8	16.1	3.0	−63	71
6.0	333.6	18.9	8.1	−63	69

[a] Equilibrium unfolding data at two different concentrations of TIM (from Figure 1) were analyzed as described by eqs 2 and 3, and the resulting fitting parameters are shown. Quality of the fits can be judged by the solid lines in Figure 1.

dimer/monomer transition. Thermodynamic parameters recovered in fits to the data at the two protein concentrations used are shown in Table 1.

(2) The extent of unfolding changed from 0.1 to 0.9 between 0.55 and 0.7 M GdnHCl. The steep dependence on GdnHCl concentration indicated high cooperativity of the transition, making the existence of populated intermediate states unlikely.

(3) Fits to the data according to eqs 2 and 3 yielded a high m value (Table 1), indicating a large increase in affinity for guanidine binding upon unfolding. Chaotropic agents are thought to interact mainly through hydrogen bonds with peptide carbonyl groups (*20*). In folded TIM, most of these groups are unavailable for interaction with guanidine since they are involved in secondary structure hydrogen bonding. Therefore, the high m value indicates significant loss of secondary structure upon unfolding. This agrees with the observation of a marked loss in ellipticity of TIM in the far UV during unfolding induced by GdnHCl (*13*).

Taken together, these observations indicate that the GdnHCl-induced transition proceeds directly from native dimers to highly unfolded (random coil) monomers. Therefore, the values of ΔG and m recovered in the fits (Table 1) apply to the overall process of dissociation and unfolding.

Figure 2 shows typical kinetic traces of unfolding and refolding of TIM at different concentrations of GdnHCl. No dependence on TIM concentration was found for the rates of refolding or unfolding (data not shown). Rate constants for unfolding and refolding were obtained through fits of eq 5 to the data. Activation free-energies ($\Delta G^{\ddagger}$) were then calculated through eq 7 and are shown as a function of GdnHCl concentration in Figure 3. From linear fits to the data (according to eq 8), $\Delta G^{\ddagger}_0$ and $m^{\ddagger}$ values were obtained (Table 2). It is noteworthy that the rate of refolding had a steeper dependence on GdnHCl concentration than the rate of unfolding (indicated by a higher m value).

DISCUSSION

In the present work, measurements of the kinetics of unfolding/refolding of TIM in GdnHCl solutions were made, and activation Gibbs free-energy changes ($\Delta G^{\ddagger}$) of the rate-limiting steps were obtained. In the following, we present a model that integrates kinetic and equilibrium data into a consistent description of subunit association/folding of dimeric TIM.

Early studies of refolding of TIM indicated the existence of a folded monomer as an intermediate between the unfolded monomer and the native dimer (*8, 9*). Furthermore, recent mutagenesis studies have demonstrated that native human TIM dimers exist in equilibrium with folded monomers, which are, in turn, in equilibrium with unfolded monomers (*11*). Based on these previous studies, we have used the following model to interpret the present data:

$$\mathrm{D} \underset{\Delta G^{\ddagger}_{\mathrm{ass}}}{\overset{\Delta G^{\ddagger}_{\mathrm{diss}}}{\rightleftharpoons}} 2\mathrm{M} \underset{\Delta G^{\ddagger}_{\mathrm{fold}}}{\overset{\Delta G^{\ddagger}_{\mathrm{unf}}}{\rightleftharpoons}} 2\mathrm{U}$$

In this model, it follows from energy conservation that the sum of activation free-energy barriers for each individual step should equal the overall ΔG of dissociation/unfolding as measured in equilibrium experiments:

$$\Delta G = \Delta G^{\ddagger}_{\mathrm{diss}} - \Delta G^{\ddagger}_{\mathrm{ass}} + 2\Delta G^{\ddagger}_{\mathrm{unf}} - 2\Delta G^{\ddagger}_{\mathrm{fold}} \quad (9)$$

From the equilibrium data shown in Figure 1, ΔG was calculated to be 69 or 71 kJ/mol for 0.6 or 6 μM TIM, respectively (Table 1). Thus, we have employed, in the calculations that follow, an average value of 70 kJ/mol for ΔG.

In our measurements, the rate-limiting step in refolding of TIM had an activation free-energy of 60 kJ/mol (Table 2). In terms of the model presented above, this activation energy could correspond to either monomer folding ($\Delta G^{\ddagger}_{\mathrm{fold}}$) or subunit association ($\Delta G^{\ddagger}_{\mathrm{ass}}$). The rate-limiting step was identified as monomer folding by the following considerations: (1) the measured refolding rates were independent of protein concentration (data not shown); (2) refolding was characterized by a large m value (Table 2), indicative of extensive formation of secondary structure in the rate-limiting step; and (3) a rate constant for rabbit TIM subunit association (k_{ass}) of 3×10^5 M^{-1} s^{-1} (from which a $\Delta G^{\ddagger}_{\mathrm{ass}}$ of 38 kJ/mol can be calculated) has been reported by Zabori et al. (*9*) from refolding studies at 0 °C.

The $\Delta G^{\ddagger}$ for the rate-limiting step of dissociation/unfolding (99 kJ/mol; Table 2) could correspond to either $\Delta G^{\ddagger}_{\mathrm{diss}}$ or $\Delta G^{\ddagger}_{\mathrm{unf}}$ in terms of the model described above. If $\Delta G^{\ddagger}_{\mathrm{unf}}$ were 99 kJ/mol, then $\Delta G^{\ddagger}_{\mathrm{diss}}$ would be 30 kJ/mol, as calculated from energy conservation (eq 9; using $\Delta G^{\ddagger}_{\mathrm{ass}} =$ 38 kJ/mol, and $\Delta G^{\ddagger}_{\mathrm{fold}} = 60$ kJ/mol; see above). This would give a negative Gibbs free-energy of dissociation ($\Delta G_{\mathrm{diss}} = \Delta G^{\ddagger}_{\mathrm{diss}} - \Delta G^{\ddagger}_{\mathrm{ass}}$) of −8 kJ/mol, in which case TIM would

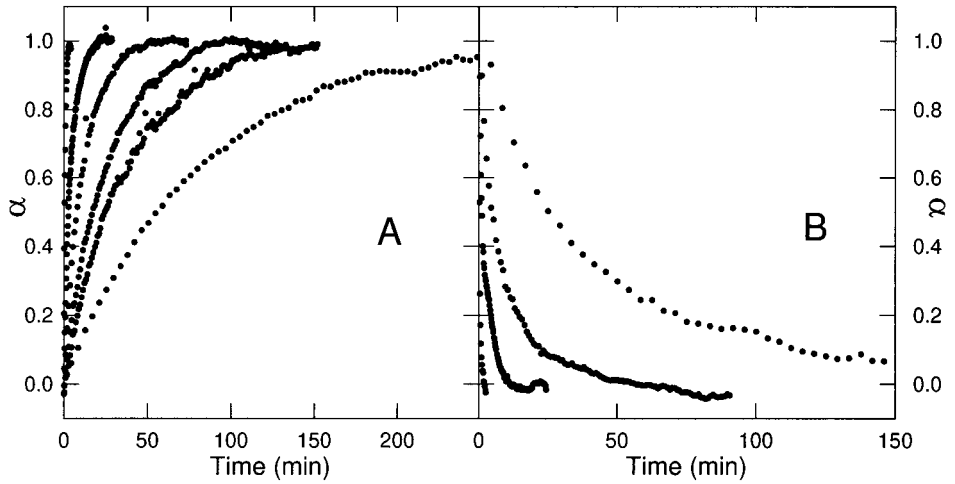

FIGURE 2: Kinetics of unfolding/refolding of TIM in GdnHCl. Panel A shows kinetics of unfolding of 0.21 μM TIM in (from left to right) 2.0, 1.5, 1.2, 1.0, 0.9, and 0.8 M GdnHCl. Panel B shows kinetics of refolding of 0.21 μM TIM in (from left to right) 0.4, 0.45, 0.55, and 0.6 M GdnHCl.

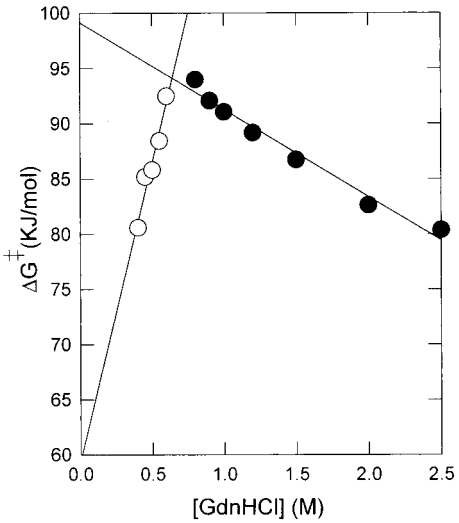

FIGURE 3: Activation free-energies for unfolding or refolding of TIM as a function of GdnHCl concentration. Activation free-energy barriers ($\Delta G^{\ddagger}$) were calculated as described in Materials and Methods for refolding (open circles) or unfolding (closed circles).

Table 2: Activation Parameters for Subunit Dissociation/Unfolding of TIM by GdnHCl[a]

	$m^{\ddagger}$ (kJ mol^{-1} M^{-1})	$\Delta G^{\ddagger}_0$ (kJ/mol)
unfolding	−8	99
refolding	54	60

[a] Values were obtained from fits according to eq 8 to the data from Figure 3.

not be a dimer. Furthermore, $m^{\ddagger}$ for unfolding was small (Table 2), suggesting moderate disruption of secondary structure in the rate-limiting step. Therefore, we identify the rate limiting $\Delta G^{\ddagger}$ of dissociation/unfolding as $\Delta G^{\ddagger}_{\text{diss}}$. Equation 9 then allows calculation of $\Delta G^{\ddagger}_{\text{unf}}$ (65 kJ/mol), completing the model depicted in Figure 4.

We note that in our model we have included $\Delta G^{\ddagger}_{\text{ass}}$ calculated from the data of Zabori et al. (*9*), which was measured at 0 °C rather than at 25 °C. Partially, the temperature dependence of rate constants is shown by the presence of T in the Arrhenius equation (eq 7). In our calculation of $\Delta G^{\ddagger}_{\text{ass}}$ and $\Delta G^{\ddagger}_{\text{fold}}$ from the data of Zabori et al. (*9*), we have covered this direct effect of temperature by

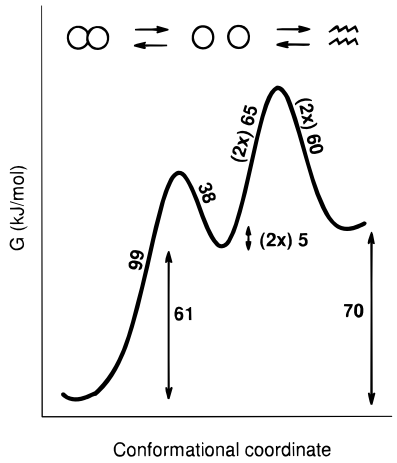

FIGURE 4: Free-energy diagram for subunit dissociation/unfolding of TIM. Activation energies are indicated directly by numbers on the energy barriers, and equilibrium free-energy changes are indicated by vertical arrows. From left to right, the diagram depicts transition from native dimers to folded monomers to unfolded monomers.

using the appropriate value for T (273 K). Implicit in the Arrhenius equation is the temperature dependence of $\Delta G^{\ddagger}$ itself. This can be estimated by the Gibbs−Helmholtz equation (*19*, *21*), adapted for activation free-energies:

$$\Delta G^{\ddagger} = \Delta G^{\ddagger}_{\text{s}} + \Delta C_p^{\ddagger}[T - T_{\text{s}} - T\ln(T/T_{\text{s}})] \quad (10)$$

where T_{s} is the temperature at which $\Delta G^{\ddagger}$ reaches its maximal value $\Delta G^{\ddagger}_{\text{s}}$ and $\Delta C_p^{\ddagger}$ is the change in heat capacity upon activation. We have not covered this dependence of $\Delta G^{\ddagger}$ on temperature, since we have no data on it. However, we would expect $\Delta C_p^{\ddagger}$ for association of folded monomers into a folded dimer to be relatively small, in which case the dependence of $\Delta G^{\ddagger}$ on temperature would be small.

In order to test our model and its underlying assumptions, we have compared its features to available data on subunit dissociation/unfolding of TIM. First, the predicted Gibbs free-energy of dissociation (ΔG_{diss}) is 61 kJ/mol (Figure 4), equivalent to $K_{\text{diss}} = 2 \times 10^{-11}$ M. This low value of K_{diss} is in agreement with previous studies by Zabori et al. (*9*), who showed that dilution down to 77 pM did not induce

monomerization of rabbit TIM. Furthermore, for human TIM, a ΔG_{diss} of 60 kJ/mol was found (*11*). The current model predicts that TIM monomers should be marginally stable, with $\Delta G_{unf} = 5$ kJ/mol (Figure 4). For human TIM, ΔG_{unf} was found to be 10.5 kJ/mol (*11*).

The unimolecular folding energy barrier ($\Delta G^{\ddagger}_{fold}$) at 0 °C was found to be 76 kJ/mol (*9*), as measured in experiments in which recovery of enzyme activity was monitored at very low protein concentrations after denaturation by GdnHCl. $\Delta G^{\ddagger}_{fold}$ in the current model at 25 °C = 60 kJ/mol (Table 2). This discrepancy may be related to the existence of additional intermediates with higher energy barriers, appearing after the relatively rapid collapse of monomer structure revealed by our fluorescence intensity measurements. Inclusion of such intermediates would lead to slower dynamics in the monomeric (un)folding part of the model. However, it would not affect the present ΔG_{diss}, $\Delta G^{\ddagger}_{diss}$, $\Delta G^{\ddagger}_{ass}$ or ΔG_{unf}, since they were established independently of $\Delta G^{\ddagger}_{fold}$.

The dynamics in dimer/monomer transition could also be slower than predicted by our model. In analogy to generally used procedures for equilibrium data (*16*), we have analyzed our kinetic data by assuming a linear dependence of $\Delta G^{\ddagger}$ on GdnHCl concentration (*17*−*19*). The linear extrapolation of ΔG as a function of GdnHCl concentration has received theoretical support from thermodynamic modeling (*22*). Inspection of the unfolding data in Figure 3 actually might indicate a slight upward curvature. This type of curvature would be compatible with other models of protein unfolding at equilibrium (*23*) and would give rise to an even higher estimate of $\Delta G^{\ddagger}_{diss}$ in the model. This would lead to slower rates of subunit dissociation. Therefore, both energy barriers in the model (for subunit dissociation/association and folding/unfolding) could be viewed as lower limiting values.

According to the present model, dimer dissociation into folded monomers should have a characteristic time of 15 h (or possibly longer, as discussed above). Folded monomers could then either reassociate into dimers or unfold. For dilute TIM solutions (micromolar or less), unfolding (with a characteristic time of 90 ms, corresponding to $\Delta G^{\ddagger}_{unf} = 65$ kJ/mol) predominates over reassociation. Therefore, the characteristic dissociation time is the minimum time required for molecules to undergo a cycle of dissociation/unfolding followed by refolding/reassociation.

In the absence of a dimer−monomer equilibrium, the unfolding/refolding cycle time for TIM monomers would be reduced to the millisecond time range. Therefore, the dimeric nature of TIM decreases the frequency of unfolding by several orders of magnitude. Since unfolded TIM is known to be susceptible to chemical modification, such as sulfhydryl oxidation and proteolysis (*8*, *13*), we conclude that dimerization greatly increases the chemical stability of TIM.

Long-lived conformational heterogeneity of TIM (on a time scale of hours to days) has been proposed based on its heterogeneous sensitivity to pressure-induced subunit dissociation/unfolding (*13*). An interconversion between two conformations of TIM with a characteristic time of 11 h at 40 °C has been described (*24*). Conformational heterogeneity could last only for times as long as or shorter than the cycle time for dissociation/unfolding. As discussed above, our model predicts a minimum lifetime of the folded state of 15 h, allowing for conformational heterogeneity that could last on this time scale. Erijman and Weber (*15*) showed a correlation between deterministic behavior (*i.e.*, reduced or lack of dependence of dissociation on protein concentration) and order of protein oligomers: dimers in general exhibit purely stochastic equilibria and large multimers exhibit completely deterministic behavior. Trimers (*25*) and tetramers (*15*) show intermediate behavior. These authors have proposed that deterministic behavior is related to persistent conformational heterogeneity of protein oligomers. Explaining these observations, a general conclusion from our present results is that oligomerization slows the dynamics of conformational recycling, thus allowing persistent conformational heterogeneity of proteins.

REFERENCES

1. Banner, D. W., Bloomer, A. C., Petsko, G. A., Phillips, D. C., Pogson, C. I., Wilson, I. A., Corran, P. H., Furth, A. J., Milman, J. D., Offord, R. E., Priddle, J. D., and Waley, S. G. (1975) *Nature 255*, 609−614.
2. Lolis, E., Alber, T., Davenport, R. C., Rose, D., Hartman, F. C., and Petsko, G. A. (1990) *Biochemistry 29*, 6609−6618.
3. Wierenga, R. K., Noble, M. E. M., Vriend, G., Nauche, S., and Hol, W. G. J. (1991) *J. Mol. Biol. 220*, 995−1015.
4. Noble, M. E. M., Zeelen, J. Ph., Wierenga, R. K., Mainfroid, V., Goraj, K., Gohimont, A.-C., and Martial, J. A. (1993) *Acta Crystallogr. D 49*, 403−417.
5. Mande, S. C., Mainfroid, V., Kalk, K. H., Goraj, K., Martial, J. A., and Hol, W. G. J. (1994) *Protein Sci. 3*, 810−821.
6. Delboni, L. F., Mande, S. C., Rentier-Delrue, F., Mainfroid, V., Turley, S., Vellieux, F. M. D., Martial, J. A., and Hol, W. G. J. (1995) *Protein Sci. 4*, 2594−2604.
7. Wierenga, R. K., Noble, M. E. M., and Davenport, R. C. (1992) *J. Mol. Biol. 224*, 1115−1126.
8. Waley, S. G. (1973) *Biochem. J. 135*, 165−172.
9. Zabori, S., Rudolph, R., and Jaenicke, R. (1980) *Z. Naturforsch. 35C*, 999−1004.
10. Borchert, T. V., Zeelen, J. Ph., Schliebs, W., Callens, M., Minke, W., Jaenicke, R., and Wierenga, R. K. (1995) *FEBS Lett. 367*, 315−318.
11. Mainfroid, V., Terpstra, P., Beauregard, M., Frère, J.-M., Mande, S. C., Hol, W. G. J., Martial, J. A., and Goraj, K. (1996) *J. Mol. Biol. 257*, 441−456.
12. Sun, A. Q., Yüksel, K. U., and Gracy, R. W. (1992) *Arch. Biochem. Biophys. 293*, 382−390.
13. Rietveld, A. W. M., and Ferreira, S. T. (1996) *Biochemistry 35*, 7743−7751.
14. Silva, J. L., and Weber, G. (1993) *Annu. Rev. Phys. Chem. 44*, 89−113.
15. Erijman L., and Weber G. (1991) *Biochemistry 30*, 1595−1599.
16. Pace, C. N. (1986) *Methods Enzymol. 131*, 266−280.
17. Matouschek, A., and Fersht, A. R. (1993) *Proc. Natl. Acad. Sci. U.S.A. 90*, 7814−7818.
18. Matouschek, A., Otzen, D. E., Itzhaki, L. S., Jackson, S. E., and Fersht, A. R. (1995) *Biochemistry 34*, 13656−13662.
19. Malecki, J., and Wasylewski, Z. (1997) *Eur. J. Biochem. 243*, 660−669.
20. Robinson, D. R., and Jencks, W. P. (1965) *J. Am. Chem. Soc. 87*, 2462−2470.
21. Becktel, W. J., and Schellman, J. A. (1987) *Biopolymers 26*, 1859−1877.
22. Schellman, J. A. (1978) *Biopolymers 17*, 1305−1322.
23. Tanford, C. (1970) *Adv. Protein Chem. 24*, 1−95.
24. Yüksel, K. U., Sun, A. Q., Gracy, R. W., and Schnackerz, K. D. (1994) *J. Biol. Chem. 269*, 5005−5008.
25. Pedrosa, C., and Ferreira, S. T. (1994) *Biochemistry 33*, 4046−4055.

BI9721593